ARTICLE OPEN

Check for updates

Heterogeneity of anti-Caspr2 antibodies: specificity and pathogenicity

Julia Su[1], Rohan Gupta[1], Scott van Hoof[2,3,4], Jakob Kreye[2,3,4,5,6], Harald Prüß[2,3,4], Benjamin Spielman[1,7], Lior Brimberg[1], Bruce T. Volpe[1], Patricio T. Huerta[1,7,8,9] and Betty Diamond[1]✉

Maternal anti-Caspr2 (Contactin-associated protein-like 2) antibodies have been associated with increased risk for autism spectrum disorder (ASD). Previous studies have shown that *in utero* exposure to anti-Caspr2 antibodies results in a phenotype with ASD-like features in male mice. Here we ask whether four newly generated antibodies against Caspr2 are pathogenic to the developing fetal brain and whether they function through similar means. Our results show that these novel anti-Caspr2 antibodies recognize different epitopes of Caspr2. *In utero* exposure to these antibodies elicits differential behavioral phenotypes in male offspring, as demonstrated in the social interaction task, as well as phenotypic alterations in the open-field and light-dark tasks. These results demonstrate variability in the antigenic specificity and pathogenicity of anti-Caspr2 antibodies which may have clinical implications.

Translational Psychiatry (2025)15:498 ; https://doi.org/10.1038/s41398-025-03677-w

INTRODUCTION

Autism spectrum disorder (ASD) affects 1 in 36 children in the United States, with a four-fold higher prevalence in males [1]. This heterogeneous neurodevelopmental disorder is characterized by impaired social interaction, communication deficits, and restricted, repetitive patterns of behavior or activities [1, 2]. ASD presents across a wide phenotypic spectrum, ranging from individuals with severe intellectual disability and seizures requiring lifelong care to those with milder presentations who live independently but experience challenges with social skills and communication [3, 4]. While the etiology of ASD is complex and likely involves both genetic and environmental factors [5, 6], increasing evidence points to a role for maternal autoantibodies in some cases. Women with autoimmune diseases have an increased risk of having a child with ASD [7–9]. Studies have revealed that a significant percentage of mothers of children with ASD possess elevated levels of anti-brain antibodies compared to mothers of typically developing children [10–15]. These antibodies have been detected through Western blot analysis for IgG reactivity to brain lysate and immunohistology for reactivity to intact brain tissue, or ELISA for specific brain antigens suggesting a potential link between maternal autoimmunity and ASD. Furthermore, animal models demonstrate that maternal anti-brain antibodies can cross the placenta and affect fetal neurodevelopment, resulting in offspring displaying ASD-like behaviors [10, 11, 16–22].

Contactin-associated protein-like 2 (Caspr2, encoded by the ASD risk gene *CNTNAP2*) has been identified as a target of some of these maternal anti-brain antibodies [10]. Caspr2, a cell adhesion protein of the neurexin family, is crucial for stabilizing the voltage-gated potassium channel complex at the juxtaparanode on the myelinated axon in the postnatal brain [16]. However, during development, Caspr2 is thought to play a role in neuronal migration and synapse stabilization [23, 24]. Our previous work demonstrated that 37% of mothers with brain-reactive antibodies and a child with ASD harbor anti-Caspr2 antibodies [10]. Interestingly, Caspr2 knockout (KO) mice exhibit an ASD-like behavioral phenotype [24–26], further implicating Caspr2 dysfunction in ASD pathogenesis.

We have previously isolated a monoclonal anti-Caspr2 IgG antibody from a mother with brain-reactive antibodies and a child with ASD. Prenatal exposure to this antibody in mice resulted in male-specific alterations in cortical development, decreased dendritic arborization in pyramidal neurons within the CA1 region of the hippocampus, and behavioral changes reminiscent of ASD, including impaired sociability, flexible learning deficits, and repetitive behaviors [10]. A subsequent study using a polyclonal antibody approach, where female mice were immunized with the extracellular portion of Caspr2, yielded similar developmental and behavioral alterations in male offspring [27]. These findings strongly support the hypothesis that maternal anti-Caspr2 antibodies can disrupt neurodevelopment, particularly in male offspring [27]. The present study investigates a panel of monoclonal anti-Caspr2 antibodies to determine their pathogenicity, binding specificity, and associated clinical phenotypes, to

[1]Feinstein Institutes for Medical Research, Northwell Health, Manhasset, NY, USA. [2]German Center for Neurodegenerative Diseases (DZNE) Berlin, Berlin, Germany. [3]Department of Neurology and Experimental Neurology, Charité-Universitätsmedizin Berlin, Corporate Member of Freie Universität Berlin, Humboldt-Universität Berlin, Berlin, Germany. [4]Helmholtz Innovation Lab BaoBab (Brain Antibody-omics and B-cell Lab), Berlin, Germany. [5]Department of Pediatric Neurology, Charité–Universitätsmedizin Berlin, corporate member of Freie Universität Berlin and Humboldt-Universität zu Berlin, Berlin, Germany. [6]Berlin Institute of Health at Charité – Universitätsmedizin Berlin, Berlin, Germany. [7]Department of Molecular Medicine, Zucker School of Medicine at Hofstra/Northwell, Hempstead, NY, USA. [8]Laboratory of Immune & Neural Networks, Feinstein Institutes for Medical Research, Manhasset, NY, USA. [9]Elmezzi Graduate School of Molecular Medicine at Northwell Health, Manhasset, NY, USA. ✉email: bdiamond@northwell.edu

Received: 24 February 2025 Revised: 2 September 2025 Accepted: 2 October 2025
Published online: 15 November 2025

determine whether there is a subset that may be particularly pathogenic. Understanding the spectrum of anti-Caspr2 antibodies will permit a more high-resolution understanding of the functionality of Caspr2 during brain development and may, in the future, allow for specific targeting of some antibodies for deletion prior to pregnancy.

METHODS

Mice and study approval

C57BL/6 mice were purchased from The Jackson Laboratory. Studies were conducted in strict accordance with the Guide for the Care and Use of Laboratory Animals of the NIH. The protocol was approved by the Institutional Animal Care and Use Committee of the Feinstein Institutes for Medical Research.

Hybridomas secreting anti-Caspr2 antibodies

Six to eight week old C57BL/6 J female mice were immunized intraperitoneal (i.p.) with 200 µg (in 50 µl of saline) of the extracellular region of human Caspr2 (Caspr2 1261 [28],) expressed using glycosylation deficient HEK293T GnTI − cells as described in [27, 28] emulsified 1:1 in Complete Freund's Adjuvant (BD Biosciences, catalog # 263810). Caspr2 1261 expends the full extracellular region of Caspr2 to residue Ser-1261 (located immediately before the transmembrane domain. Mice were boosted 3 weeks after the initial immunization with 200 µg of Caspr2 (emulsified 1:1 in Incomplete Freund's Adjuvant (BD Biosciences, catalog # 263810), via intraperitoneal injection. Antibody titers were checked with a HEK Cell Based Assay as described [8, 13, 15]. Three days after the booster, mice were euthanized, and spleens were harvested. Splenocytes were extracted using the balloon technique and transferred to a 50-mL conical tube and placed on ice for 5 min to allow debris to separate from cells by sedimentation. To remove red blood cells from the splenocyte mixture, the mixture was pelleted by centrifugation at 400 g for 5–10 min. The pellet was loosened by flicking, and 5 mL of cold NH_4Cl (0.01 mL, 7 M pH 7) was added. After 10 min on ice, 10 mL of cold DMEM was added slowly to stop the lysis reaction. Splenocytes were combined with myeloma cells. Myeloma cells were grown separately in preparation for fusion with splenocytes (myeloma lines were obtained from Dr. Matthew Scharff, Albert Einstein College of Medicine). Originally, P3-X63-Ag8 cells were used but NSO-BCL2 cells were used to improve the efficiency of generating hybridomas that produced antibodies against Caspr2. For maintaining fusion partner hybridoma lines P3-X63-Ag8 and NSO-BCL2, cells were grown in complete medium and fed every 2–3 days and split every other feed at 1:5 dilution. Fusions were performed as described [22].

Caspr2-binding ELISA

Supernatant from wells in the 96-well plates with semiconfluent growth of hybridoma cells were assayed by ELISA to determine which wells have anti-Caspr2 antibody producing hybridomas. For simplicity, we used the same name for the hybridoma cell line and the antibody it produced. For ELISA, Costar (Cat No. 3690) half area, 96-well plates were coated with 5 µg/mL of human extracellular portion of Caspr2 protein overnight at 4°C. Plates were washed with 1x PBS before blocking with 3% Fetal Bovine Serum (FBS) in 1x PBS for 1 h at 37°C. Plates were then washed 6x with 1x PBS-0.1% Tween-20 before incubation with the secondary antibody, a 1:1000 dilution of Goat Anti-Mouse IgG(H + L)-AP (Southern Biotech, Cat No. 1036-04). Plates were washed 6x with 1x PBS-0.1% Tween-20, incubated with developing solution (AP substrate (Sigma-Aldrich, Cat No S0942), in 0.001 M $MgCl_2$ and 0.05 M $NaHCO_3$), and read at multiple time points (30 min, 45 min, and 1 h) at a wavelength of 405 nM on a 1430 Multilabel Counter Spectrometer (PerkinElmer). Each sample was assayed in duplicate. Each sample that had an average absorbance value greater than the negative control was considered positive and the cells expanded to 24-well plate for future cloning.

Cloning of hybridomas in soft agarose

Hybridomas producing anti-Caspr2 antibody were cloned as described [29].

Hybridoma cell culture maintenance

After cloning and confirmation of anti-Caspr2 antibody secretion by ELISA, positive hybridomas were expanded to Fisherbrand™ Surface Treated Sterile Tissue Culture Flasks, Vented Cap (Fisher Scientific, Cat No FB012939) and were transitioned to grow in Gibco™ Hybridoma-SFM medium (ThermoFisher Scientific, Cat No 12045076) following a stepwise process (i.e.75% complete medium/25% Hybridoma-SFM for a week, 50% complete medium/50% Hybridoma-SFM for a week, and 25% complete medium /75% Hybridoma-SFM for week). Cells were fed every 2–3 days and split every other feed at a 1:5 dilution.

Antibody purification

Supernatant from hybridoma cultures was collected, centrifuged at 200xg for 5 min (to pellet out cellular debris), and added to Pierce™ Protein G agarose (Thermo Fisher, Cat No. 20399) that had been washed with 1x PBS. Supernatant with agarose was incubated on a rotator overnight at 4 °C. The next day, the mixture was centrifuged at 1000 rcf for 10 min to pellet the agarose. The agarose was washed twice with 1x PBS. Anti-Caspr2 antibody was eluted from agarose using 0.1 M glycine (pH 3.0) into Eppendorf tubes that were preloaded with 1 M Tris-HCl to neutralize the glycine to pH 7.0. The elution fractions with IgG were pooled and dialyzed overnight at 4 °C using a Slide-A-Lyzer Dialysis Cassette (Thermo Fisher, Cat No. A52971) to exchange the antibody buffer to 1x PBS. Antibody concentration was measured using Nanodrop Spectrophotometer and then stored at −20 °C.

Sequencing of heavy and light chains of hybridomas

RNA from hybridoma cells was extracted using Qiagen RNeasy Kit (Qiagen) following manufacturer's instructions. cDNA was generated from extracted RNA using iScript™ cDNA Synthesis Kit (Bio-Rad) following manufacturer's instructions. The cDNA served as the PCR template for cloning heavy and light chain sequences to confirm the presence of PCR product, and the band of the right size was excised and cleaned using QIAquick PCR Purification Kit (Qiagen). The PCR product was then ligated into TOPO-TA vector (Invitrogen) following the manufacturer's instructions and then transfected into One Shot™ TOP10 Chemically Competent *E. coli* bacteria (Invitrogen). Bacteria were plated on ampicillin LB agar plates and placed upside down in 37 °C incubator overnight. The next day colonies were picked and sent to Azenta Life Sciences for Sanger sequencing. The sequencing results were then aligned against the IMGT® database to determine specific heavy and light chains.

IgG binding ELISA

Costar (Cat No. 3690) half area, 96-well plates were coated with 10 µg/mL of unlabeled anti-mouse IgG, IgG1, IgG2b, IgG2c, IgG3 overnight at 4°C. Plates were blocked with 3% FCS for 1 h at 37 °C. Anti-Caspr2 antibodies were tested against each isotype by adding supernatant to the ELISA plate followed by an AP conjugated antibody to the same isotype Goat anti-mouse IgG1 (Southern biotech # 1070-04), Goat anti-mouse IgG2a, (Southern biotech # 1081-04), Goat anti-mouse IgG2b (Southern biotech # 1090-04), and Goat anti-mouse IgG3 (Southern biotech # 1100-04). Plates were incubated with developing solution (AP substrate, Sigma-Aldrich, Cat No S0942, in 0.001 M $MgCl_2$ and 0.05 M $NaHCO_3$), incubated at 37 °C, and read at 30 min at a wavelength of 405 nM on a 1430 Multilabel Counter Spectrometer (PerkinElmer).

Caspr2 binding cell-based assay

HEK cells (5,000,000) were seeded in 100 × 20 mm Falcon® Tissue Culture-treated dish (Fisher Scientific, Cat no 353003) for each transfection. At 24 h after plating, cells were transfected via Fugene (Promega, Cat no #E269A) with human Caspr2 tGFP (Origine, RG210836) construct, mouse Caspr2 tGFP (Origine, MG221930) construct, or nothing. At 48–72 h after transfection, the live cell-based assay was performed as described [10, 27].

Timed pregnancies via trio breeding. For timed pregnancy, two females and one male were housed together for 14 h. The time when the male mouse was removed from the cage was designated embryonic (E) day 0.5. Pregnant females were randomly chosen to be injected with Caspr2 monoclonal antibody or isotype control(200 µ g). IgG was administered by retro-orbital injection to time-pregnant mice under light anesthesia at E13.5.

Generation of adult mouse brain sections

Male C57BL/6 mice (12–20 weeks old) underwent transcranial perfusion following standard protocols. For PFA fixed sections, mice were first

perfused with pre-perfusion solution containing 0.5% sodium nitrite, 0.9% sodium chloride, and 0.1% heparin followed by 4% PFA diluted in 0.2 M PB. Brains were carefully removed from the skull and put into vials containing 20 mL of 4% PFA solution and post-fixed for 2 h. Brains were transferred to 30% sucrose solution for 24–48 h before freezing in Tissue-Tek® OCT compound (Sakura). Brains were stored in −80 °C until sectioning. For snap frozen brain sections, mice were perfused with pre-perfusion solution prior to brain removal, brains were then snap frozen in −40 °C methylbutane and stored at −80 °C until sectioning. For both PFA-fixed and snap frozen brains, 14-µm sections were cut on a cryostat and mounted onto Fisherbrand Superfrost Plus Microscope Slides (FisherScientific, Cat No 22-037-246). Sections were stored at −80 °C until staining.

Generation of E15.5 mouse sections

Dams with timed pregnancies were euthanized using CO_2 following IACUC guidelines on day E15.5. Embryos were extracted via c-section and were washed in ice cold Gibco™ HBSS (ThermoFisher Scientific, Cat No 14175095) prior to fixation in 4% PFA, 4% sucrose for 4 h at room temperature. Embryos were incubated in a sucrose gradient (10% sucrose for 45 min at 4 °C, 20% sucrose for 2 h at 4 °C, 30% sucrose overnight at 4 °C) prior to freezing in Tissue-Tek® OCT compound (Sakura). Full embryo, 12-µm sagittal sections were cut on the cryostat and mounted onto Fisherbrand Superfrost Plus Microscope Slides (FisherScientific, Cat No 22-037-246). Sections were stored at −80 °C until staining.

Generation of mouse primary neuronal cultures. Neuronal cultures we generated as described [30].

Immunohistochemistry on PFA fixed adult brain sections

Sections were rehydrated in 1x PBS for 5 min twice prior to antigen retrieval in 10 mM sodium citrate buffer at 95 °C for 2 min. Sections were washed in 1x PBS for 5 min and blocked in 3% BSA in 0.1% Triton X-100 at room temperature for 1 h, incubated with 10 µg/mL of hybridoma generated anti-Caspr2 antibodies overnight at 4 °C, washed with 1x PBS-0.1%Tween-20, and then incubated with secondary antibody anti-mouse Alexa Fluor 488 (ThermoFisher Scientific, Cat No A32723, 1:400) for 1 h at room temperature, protected from light. Sections were then stained with 0.5 µg/mL DAPI for 5 min prior to being coverslipped with DAKO mounting medium (Agilent, Cat No S3023), and imaged (Zeiss,Axioimager Z1, N.A. = 0.8).

Immunohistochemistry on snap frozen adult brain sections

Sections were fixed in 95% EtOH in −20 °C for 30 min, followed by 1 min in acetone at −20 °C. Sections were blocked in 3% BSA in 1x PBS-0.1% Triton X-100 at room temperature for 1 h, incubated with 10 µg/mL of hybridoma generated anti-Caspr2 antibodies overnight at 4 °C, washed with 1x PBS-0.1% Tween-20, and incubated with secondary antibody anti-mouse Alexa Fluor 488 (ThermoFisher Scientific, Cat No A32723, 1:400) for 1 h at room temperature, protected from light. Sections were stained with 0.5 µg/mL DAPI for 5 min prior to being coverslipped with DAKO mounting medium (Agilent, Cat No S3023), and imaged (Zeiss Axioimager Z1, N.A. = 0.8)

Immunohistochemistry on mouse primary neuronal cultures

DIV14 neuronal cultures were fixed in 4% sucrose, 4% PFA at room temperature for 10 min. Cells were blocked with 4% BSA in 1x PBS for 30 minutes at room temperature. Cells were incubated in primary antibody; 10 µg/mL of anti-Caspr2 (P11G7, P9C7, P6B2, or P13F4) and a commercial anti-Caspr2 antibody (EMD Millipore, Cat No ABN1380, 1:1000) diluted in blocking buffer overnight at 4 °C. Cells were incubated in secondary antibodies; anti-mouse Alexa Fluor 488 (ThermoFisher Scientific, Cat No A32723, 1:400) and anti-rabbit Alexa Fluor 594 (ThermoFisher Scientific, Cat No A32740, 1:400) diluted in blocking buffer for 1 h at room temperature, protected from light. Cells were incubated with DAPI (ThermoFisher Scientific, Cat No 62248, 0.5 µg/mL) 5 min at room temperature, protected from light. The glass coverslips were then mounted onto Fisherbrand Superfrost Plus Microscope Slides (FisherScientific, Cat No 22-037-246) using DAKO mounting medium (Agilent, Cat No S3023), sealed with clear nail polish, and then visualized by microscopy. Microscopy images were taken at 20x on Zeiss Brightfield Microscope using a Colibri LED system.

Generation of behavioral cohorts

Timed pregnancies were set up by trio breeding as described above. At E13.5, 200 µg of anti-Caspr2 antibody (P11G7, P9C7, P6B2, or P13F4) or an isotype control antibody was injected into pregnant dam via retroorbital injection. Pregnant dams were separated and single housed. At least 5 litters with each antibody treatment were generated so at least 8 mice were in each treatment group segregated by gender. After weaning, mice were transferred to the reverse light cycle room for behavioral testing.

Behavioral assessments

Mice exposed to anti-Caspr2 antibodies *in utero* were housed under a reversed dark (9:00–21:00) and light (21:00–9:00) cycle, with *ad libitum* access to food and water. All manipulations were conducted during the dark phase, at least 1 h after turning the lights off. At 8–9 weeks of age, mice were handled 3x (15 min sessions) on separate days. One week later, they underwent a baseline assessment that measured body weight, coat, grip strength, body tone, reflexes, and sickness behavior. Behavioral assessments were performed at 12–15 weeks of age, following this sequence: light-dark-chamber task (12 weeks of age), open-field task (13–14 weeks of age), and social interaction task (15 weeks of age). Experiments were conducted and analyzed according to randomly assigned cage numbers that did not indicate antibody exposure. Animals from different litters were distributed across experimental cohorts to control for litter effects. During experimentation, the investigator was blinded to the antibody exposure status of the mice. Environmental conditions (lighting, temperature, background noise) were strictly controlled and consistent across all testing sessions. All the tasks were recorded with a centrally placed video camera directly above each arena which fed the signal to the tracking software (EthoVision XT 14.0, Noldus, Attleboro, MA, USA). Eight to >20 mice in each cohort were studied. This number has revealed differences in prior studies [10, 27].

Light-dark chamber task

This test measured the mice's natural aversion to bright light. Each mouse was placed for 10 min in the Noldus light-dark box (Noldus, Attleboro, MA, USA),which consisted of a chamber with a large open compartment that was highly illuminated (800 lux, measured with Lutron LX-102 light meter) and a small dark compartment (5–15 lux). The Noldus light-dark box is made from IR translucent materials, which in combination with the IR backlight and IR-sensitive camera, makes the apparatus suited for video tracking with EthoVision software. The apparatus was cleaned prior to each trial with 70% ethanol followed by water and wiped dry.

Open field task

This test examined locomotor activity and exploratory behavior by placing the mice in the center of a square arena (40 × 40 cm) with gray walls (35 cm high) and allowing them to freely explore the chamber during two sessions (15 min each) separated by ~2 h. The sessions were recorded with a centrally placed video camera directly above the arena which fed the signal to EthoVision software, which was used for automated analysis of animal behaviors including distance traveled, velocity, time spent moving, time spent in the center of the arena (20×20 cm^2). The arena was cleaned in between each trial with 70% ethanol followed by water and wiped dry.

Social interaction task

Prior to beginning the task, the "stimulus" mice were lightly anesthetized, shaved, and their backs were colored with a non-toxic marking ink, allowing these mice to be differentiated from the experimental mice. Each stimulus mice was used only once per day but they were re-used across testing days. Moreover, each stimulus-mouse was placed into a chamber (30×30 cm, 40 cm high) for 20 min to familiarize itself with the environment. For the test proper, the stimulus mouse was introduced to the chamber together with an experimental mouse and the two animals were allowed to interact for 10 min. The social interaction module of the EthoVision software was used to detect body contact, based on the body contours of the two animals.

Golgi-cox staining and sholl analysis

Brains were prepared for morphometric analysis, as previously described [30, 31], with Rapid GolgiStain™ Kit (FD Neuro Technologies), a silver staining method that permits visualization of entire neurons. Comparable sections across all animals were imaged (Zeiss Axioimager Z1,N.A. = 0.75, z-step=5 µm). There were 5 animals in each group (except for the P11G7 group which had 3 mice and the controls in the IgG1 and IgG2 group which had 4), and for each animal there were at 8–12 neurons traced and

Table 1. Summary of observations of anti-CASPR2 antibodies and their respective isotype control.

Antibody	Adult brain slices (PFA)	Adult brain slices (snap frozen)	E15.5 sections	Primary neuronal culture	HEK cell based assay (M=mouse) (H=human)	Caspr 2 domain specificity	Behavior	Dendritic Length
P11G7 (IgG1)	Yes	Yes	Yes	Yes	Yes (M/H)	discoidin	No phenotype	No differences
P9C7 (IgG1)	No	Yes	Yes	No	Yes (M/H)	discoidin	Reduced social interaction Reduced time in center in open field task	No differences
P13F4 (IgG2b)	Yes	Yes	Yes	Yes	Yes (M/H)		Reduced time in center in open field task Hyperactivity	No differences
P6B2 (IgG2b)	Yes	Yes	No	Yes	Yes (M/H)	None	Reduced social interaction	Reduced-See Fig. 2 and Fig. 2 Legend
P3.6.2.8.1 (IgG1 control)	No	No	No	No	No	None		
MPC11 (IgG2b control)	No	No	No	No	No			

measured using Neurolucida® (MBF Bioscience). Dendritic length measurements were compiled according to a Sholl analysis [31] for a linear mixed model analysis (R program v.3.1-168 with Rstudio) to test for group differences and generate interclass correlation values.

Anti-caspr2 antibody target domain identification

HEK293T cells were transfected with human full-length Caspr2 cDNA or mutant constructs, each missing one of the domains. These mutant constructs were generated as described previously [32] In short, eight deletion constructs were generated using Q5 Site-Directed mutagenesis kit (NEB). The specific amino acid residues deleted in each construct were defined based on the domain boundaries annotated in UniProtKB (accession number: [Q9UHC6]). No additional linkers were inserted between adjacent domains following deletion. An additional construct was generated containing only the discoidin domain. Reactivity against these constructs was then tested through cell-based assay with live-staining using established methods [32]. In brief, 48 h after transfection, antibodies were diluted to 5 µg/ml in growth medium (DMEM+Glutamax, 10% FBS, 1% Streptomycin/Penicillin, 1% MEM non-essential amino acid solution) and added to the cells. After 1 h incubation (37 °C), medium was removed, and cells were fixed with 4% PFA. After washing, Alexa Fluor 488 coupled goat anti-human antibody (1:1000; Dianova CAT#:109-545-003) was added and left to incubate for 2 h at room temperature. Images were then obtained using widefield imaging on a Leica SPE. Reactivity against the discoidin domain was confirmed through a CBA using an additionally generated construct containing only the discoidin domain.

RESULTS

Generation of anti-caspr2 antibodies

Four unique monoclonal anti-Caspr2 antibodies were generated via hybridoma technology from spleen cells of female mice immunized with the extracellular domain of human Caspr2. Two IgG1 antibodies, termed P9C7 and P11G7, were derived using the P3-X63-Ag8 myeloma line while two IgG2b antibodies, termed P6B2 and P13F4, were generated using the NSO-BCL2 (Bcl-2 overexpressing) myeloma line (Table 1).

Characterization of IgG1 anti-Caspr2 antibodies, P11G7 and P9C7

Sequence analysis confirmed the unique heavy and light chain sequences of P11G7 and P9C7 (Fig. 1A). Moreover, ELISA analysis showed that both molecules were IgG1 antibodies (Fig. 1B). Importantly, P11G7 and P9C7 displayed robust binding to human and mouse Caspr2 expressed in HEK293 cells, while an IgG1-matched isotype control (CON1) showed null binding (Fig. 1C, *top*). P11G7 and P9C7 also recognized human and mouse Caspr2 in GnTI-HEK293 cells (lacking complex glycosylation) (Fig. 1C, *bottom*). In mouse brain tissue, P11G7 bound to PFA-fixed adult, snap-frozen adult, and PFA-fixed E15.5 embryonic brain sections (Fig. 1D, *top*). P9C7 exhibited binding to snap-frozen adult and E15.5 brain sections (Fig. 1D, *bottom*). Both antibodies also bound to Caspr2 in primary neuronal cultures, colocalizing with a commercial anti-Caspr2 antibody (Fig. 1E).

The model of prenatal exposure to maternal antibodies was used in three groups of offspring: those from dams exposed to P11G7, dams exposed to P9C7, and dams exposed to CON1. At a baseline level, no significant differences in body weight, coat, grip strength, body tone, reflexes, or sickness behavior were observed in male or female offspring exposed to any of the anti-Caspr2 antibodies compared to isotype controls. Moreover, female offspring of all groups showed no significant differences in the social interaction, open field, and light-dark tasks (Supplemental Fig. 1). Importantly, P9C7 male offspring displayed reduced time interacting in the social task (Fig. 1F, mean ± SEM, CON1 = 177.15 ± 6.36 s; P9C7 = 142.72 ± 6.74 s; $q = 5.46$, $P = 0.0008$, ANOVA with Tukey test) and decreased exploration of the center of the chamber (Fig. 1F, time in center, CON1 = 126.43 ± 5.73 s; P9C7 = 97.03 ± 5.37 s; $q = 4.95$, $P = 0.0025$) but no difference in distance moved in the open field task (Fig. 1F, CON1 = 6679.5 ± 140.96 cm; P9C7 = 6669.28 ± 220.87 cm; $q = 0.06$,

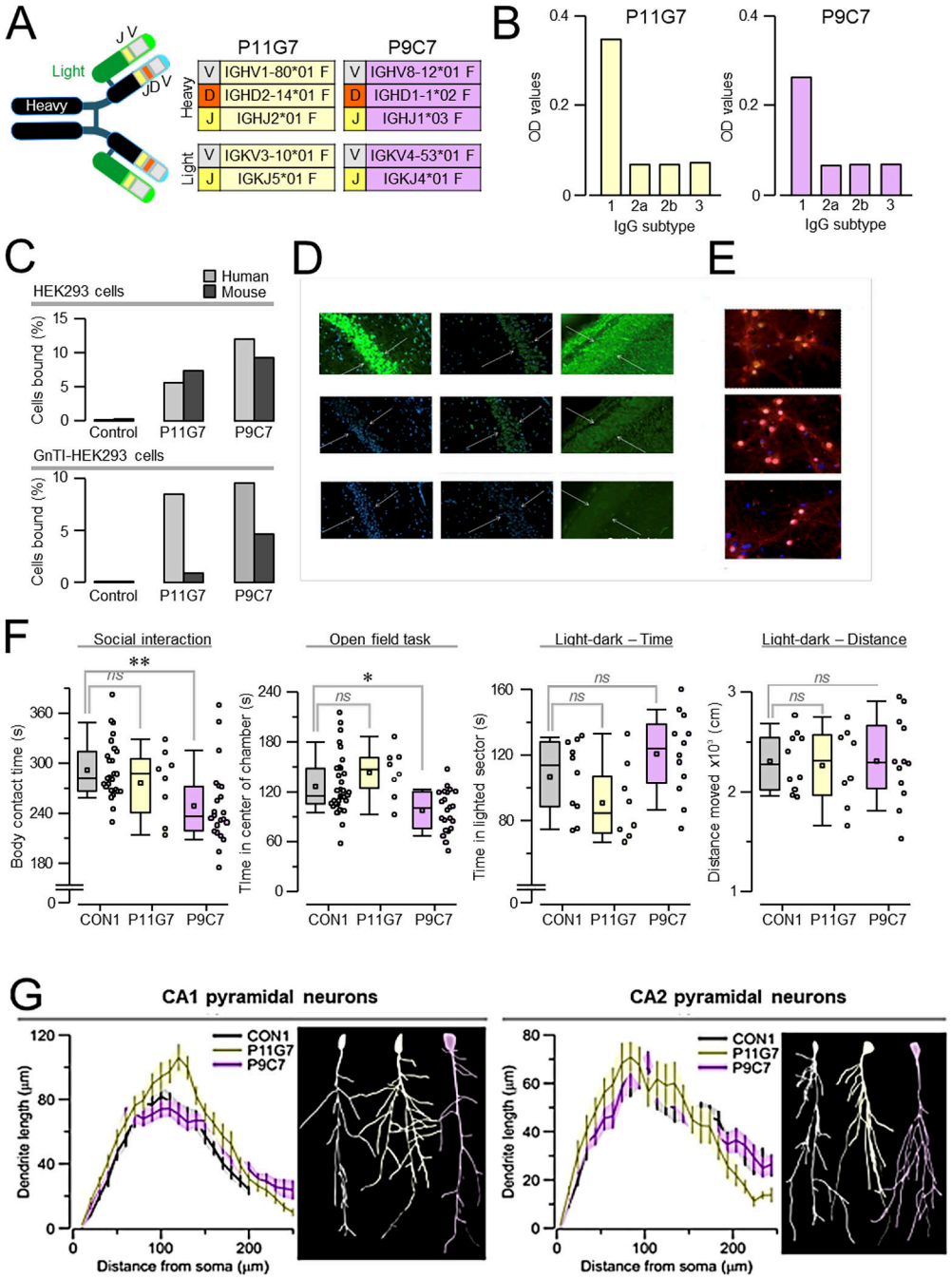

Fig. 1 IgG1 anti-Caspr2 antibodies. A Diagram of the structure of P11G7 and P9C7 with their unique sequences for the heavy and light chains. **B** Isotype determination with a sandwich ELISA done by coating a plate with various anti-IgG isotype subtypes, adding purified antibody to each well, and measuring their optical density (OD). P11G7 and P9C7 are clearly IgG1 isotype. **C** Anti-Casp2 binding on HEK293 cells (top) and GnTI-HEK293 cells (bottom). P11G7 and P9C7 bind to both human Casp2 and mouse Caspr2 compared to an IgG1-matched isotype control (CON1). **D** Binding of P11G7 (10 μg/mL) and P9C7 (10 μg/mL) to adult mouse brain sections, PFA-fixed (first column), snap-frozen (second column) and E15.5 whole embryo sections (third column). P11G7 (top row) binds to all sections, whereas P9C7 (second row) binds to snap-frozen and embryonic sections but not PFA-fixed sections. IgG1 isotype control third row. Representative images of the CA1 region of the hippocampus (adult, first and second column) and cortical plate (E15.5, third column) at 20x. **E** Binding of P11G7 (10 μg/mL) and P9C7 (10 μg/mL) to primary neuronal cultures (fixed at DIV14) stained with primary antibodies. Hybridoma anti-Caspr2 antibodies are labeled in green, a commercial anti-Caspr2 antibody (ABN1380) in red, and their co-localization in yellow. Images (P11G7 top, P9C7 middle, IgG1 isotype control bottom) taken at 40x. **F** Assessment of male mice exposed to anti-Caspr2 antibodies *in utero* reveals that mice in the P11G7 group have no differences in any of the tasks compared to the CON1 group, while mice in the P9C7 group has less body contact with an unfamiliar mouse in the social interaction task, and less time in the center of the chamber in the open field task. Statistical testing done with ANOVA followed by Tukey post-hoc test. (**G**) Sholl analysis of pyramidal neurons from the CA1 and CA2 regions of the hippocampus reveals no significant differences in dendritic length between the groups. Insets (at right in each panel) show representative tracing of CA1 and CA2 neurons.

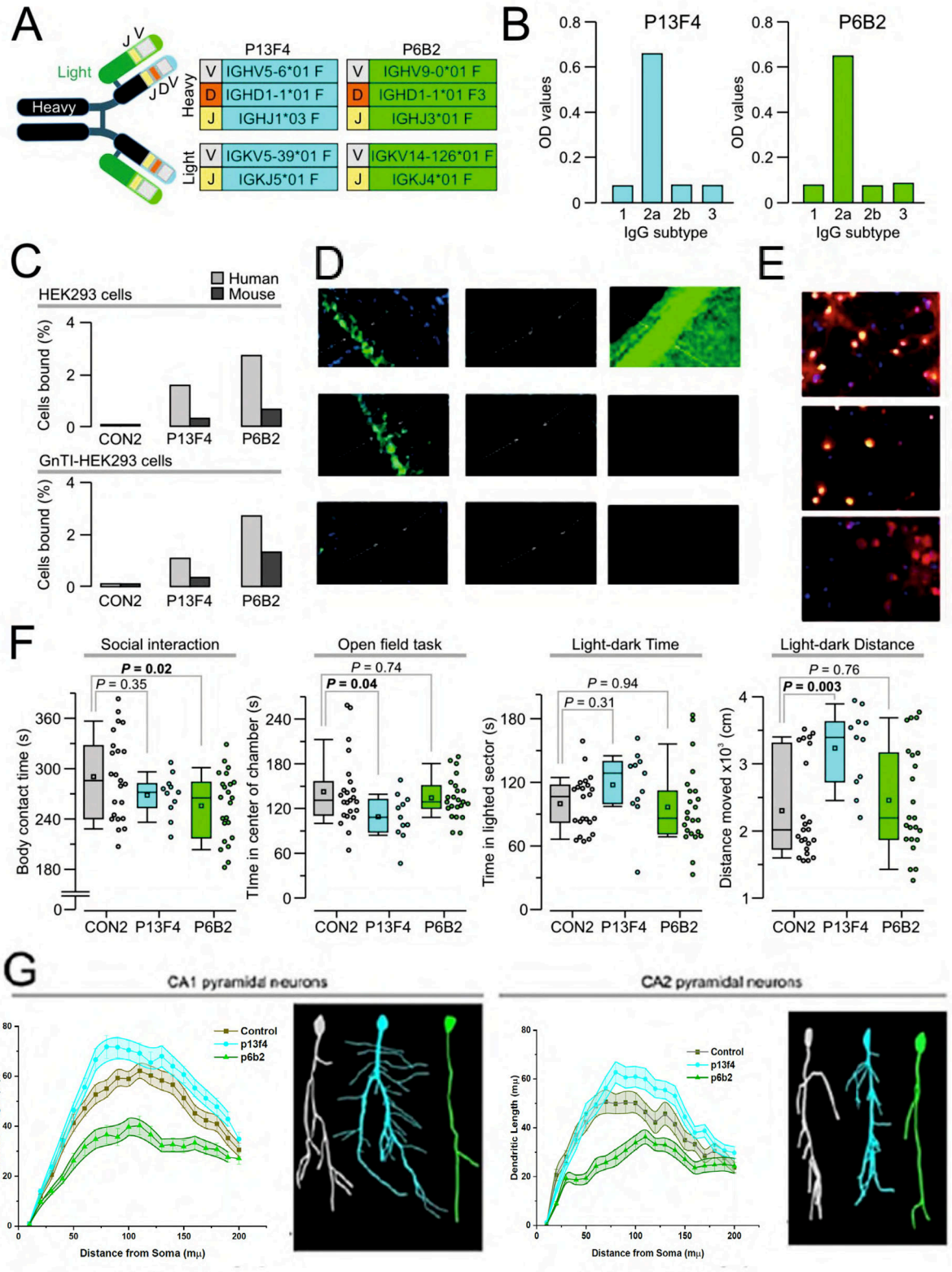

$P = 0.99$). Conversely, *in utero* exposure to P11G7 did not result in significant changes during social interaction (Fig. 1F, P11G7 = 195.24 ± 7.29 s; $q = 2.06$, $P = 0.32$) and open field behavior (Fig. 1F, time in center, P11G7 = 142.71 ± 10.48 s; $q = 1.89$, $P = 0.38$; distance moved, P11G7 = 6159.68 ± 206.34 cm; $q = 2.11$, $P = 0.3$) in male offspring. Additionally, no differences were observed in the in the light-dark task for time spent in the lighted sector (Fig. 1F, CON1 = 106.91 ± 7.17 s; P9C7 = 120.96 ± 7.33 s; $q = 1.94$, $P = 0.37$; P11G7 = 91.19 ± 8.29 s; $q = 1.95$, $P = 0.36$) and the distance moved (Fig. 1F, CON1 = 2302.24 ± 93.86 cm; P9C7 = 2310.23 ± 124.06 cm;

Fig. 2 IgG2 anti-Caspr2 antibodies. A Diagram of the structure of P13F4 and P6B2 with their unique sequences for the heavy and light chains. **B** Isotype determination with a sandwich ELISA done by coating a plate with various anti-IgG isotype subtypes, adding purified antibody to each well, and measuring their optical density (OD). P13F4 and P6B2 are IgG2 isotype. **C** Anti-Casp2 binding on HEK293 cells (top) and GnTI-HEK293 cells (bottom). P13F4 and P6B2 bind preferentially to human Casp2 and less to mouse Caspr2 compared to the null binding of an IgG2-matched isotype control (CON2). **D** Binding of P13F4 (10 μg/mL) and P6B2 (10 μg/mL) to adult mouse brain sections, PFA-fixed (first column), snap-frozen (second column) and E15.5 whole embryo sections (third column). In brain tissue, P6B2 (second row) binds only to PFA-fixed adult sections, whereas P13F4 (first row) binds to both PFA-fixed adult and E15.5 embryonic sections. IgG2b isotype control third row. Representative images of the CA1 region of the hippocampus (adult, first and second column) and cortical plate (E15.5, third column) at 20x. **E** Binding of P13F4 (10 μg/mL) and P6B2 (10 μg/mL) to primary neuronal cultures (fixed at DIV14) stained with primary antibodies. Hybridoma anti-Caspr2 antibodies are labeled in green, a commercial anti-Caspr2 antibody (ABN1380) in red, and their co-localization in yellow. Images (P13F4 top, P6B2 middle, IgG2b isotype control bottom) taken at 40x. **F** Assessment of male mice exposed to anti-Caspr2 antibodies *in utero* reveals that mice in the P13F4 group have normal behavior in the social interaction task but less time in the center of the chamber during the open field task and more distance covered in the light-dark box task. Mice in the P6B2 group show less body contact with an unfamiliar mouse in the social interaction task. Statistical testing done with ANOVA followed by Tukey post-hoc test. **G** Sholl analysis of pyramidal neurons from the CA1 and CA2 regions of the hippocampus reveals that P6B2-exposed males have significantly shorter dendrite length when compared to male mice exposed to isotype control in both CA1($P < 0.007$, ICC=0.174) and CA2 neurons ($P = 0.0084$, ICC = 0.214). Insets (at right in each panel) show representative tracing of CA1 and CA 2 neurons.

$q = 0.07$, $P = 0.99$; P11G7 = 2259.37 ± 138.06 cm; $q = 0.34$, $P = 0.96$) for any of the antibody-exposed groups.

Previously, we showed that male offspring exposed to the C6 anti-Caspr2 antibody had reduced exploration during repeated trials of the open field task [29], which prompted us to perform a second session in all groups. Analysis of both trials with repeated measures ANOVA (RMANOVA) revealed that P9C7 males spent significantly lower time than CON1 males in the chamber's center (Supplemental Fig. 2, $q = 3.99$, $P = 0.017$, RMANOVA with Tukey test) but moved similar distance ($q = 1.05$, $P = 0.74$). P11 G7 males were similar to CON1 mice in terms of time in center ($q = 1.23$, $P = 0.66$) but had significantly different distance moved ($q = 4.29$, $P = 0.0095$).

A neuroanatomical approach, with Golgi-Cox staining followed by Sholl analysis, was applied to quantify the dendritic arborization of pyramidal neurons in the CA1 and CA2 regions of the hippocampus. Surprisingly, no significant changes in dendritic length were observed in the CA1 or CA2 hippocampal regions of P9C7 or P11G7-exposed males (Fig. 1G).

Characterization of IgG2b anti-Caspr2 antibodies, P13F4 and P6B2

Heavy and light chain sequences were obtained for P13F4 and P6B2 (Fig. 2A). Moreover, ELISA analysis showed that both molecules were IgG2 antibodies (Fig. 2B). Moreover, P13F4 bound more robustly to human than mouse Caspr2 in both HEK293 and GnTI-HEK293 cells (Fig. 2C), suggesting a stronger binding selectivity for human Caspr2. P6B2 showed a similar pattern, binding better to human Caspr2 than mouse Caspr2 in HEK294 and GnTI-HEK293 cells (Fig. 2C). Importantly, an IgG2-matched isotype negative control (CON2) showed null binding to HEK293 and GnTI-HEK293 cells (Fig. 2C). In brain tissue, P6B2 bound only to PFA-fixed adult sections, whereas P13F4 bound to both PFA-fixed adult and E15.5 embryonic sections (Fig. 2D). Both P6B2 and P13F4 bound to Caspr2 in neuronal cultures (Fig. 2E).

Male offspring exposed *in utero* to P13F4 exhibited normal time interacting in the social interaction task (Fig. 2F, CON2 = 290.21 ± 10.6 s; P13F4 = 268.19 ± 7.65 s; $q = 1.98$, $P = 0.35$, ANOVA with Tukey test) but decreased time exploring the center of the chamber (Fig. 2F, CON2 = 142.68 ± 10.6 s; P13F4 = 109.04 ± 9.27 s; $q = 3.43$, $P = 0.04$) and more distance moved (Fig. 1F, CON2 = 6241.11 ± 166.5 cm; P13F4 = 7319.75 ± 263.32 cm; $q = 5.1$, $P = 0.002$) in the open-field task. P13F4 males also showed hyperactivity in the light-dark box task in terms of distance moved (Fig. 2F, CON2 = 2302.42 ± 152.91 cm; P13F4 = 3233.42 ± 177.73 cm; $q = 4.88$, $P = 0.003$). Analysis of the open-field task as repeated sessions further demonstrated that P13F4 males behaved significantly different than CON2 mice (Supplemental Fig. 2, time in center, $q = 5.1$, P = 0.002; distance moved, $q = 4.27$, P = 0.011).

Remarkably, P6B2-exposed males displayed reduced social interaction (Fig. 2F, P6B2 = 255.58 ± 8.43 s; $q = 3.87$, $P = 0.022$) and no behavioral changes in the open field task (Fig. 2F, time in center, P6B2 = 134.48 ± 5.75 s; $q = 1.04$, $P = 0.74$; distance moved, P6B2 = 6502.25 ± 804.61 cm; $q = 1.53$, $P = 0.53$) and the light-dark task (Fig. 2F, P6B2 = 2457.62 ± 165.76 cm; $q = 1.01$, $P = 0.76$). Finally, P6B2-exposed males had significantly decreased dendritic length when compared to controls within CA1 ($P = 0.007$,ICC = 0.174) and CA2 ($P = 0.0084$,ICC = 0.214) neurons (Fig. 2G).

Of importance, the differences in behavioral assays does not relate to differences in placental transfer of the antibodies as IgGI and IgG2b cross the placenta equally well (TiBiochem.)

Anti-Caspr2 antibodies bind to different epitopes on Caspr2

To determine the target domain recognized by each anti-Caspr2 antibody, HEK293T cells were transfected with either the full length or a mutant construct encoding for the human Caspr2 protein. Each mutant construct contained the deletion of one of the eight extracellular domains or had only a single domain (Fig. 3A). These epitope mapping studies using human Caspr2 deletion mutants revealed that both P11G7 and P9C7 targeted the discoidin domain (Fig. 3B), as they bound to every mutant Caspr2 construct except the construct lacking the discoidin domain (ΔDisc). Also, both P11G7 and P9C7 bound to a construct containing only the discoidin domain (Fig. 3C).

In contrast, P6B2 and P13F4 did not bind to any of the deletion mutants. (Fig. 3B, C), consistent with the preferential binding of P6B2 to mouse Caspr2 and preferential binding of P13F4 to Caspr2 in the absence of complex glycosylation.

DISCUSSION

Our previous work identified anti-Caspr2 IgG in a substantial proportion (37%) of mothers with anti-brain antibodies and a child with ASD, suggesting Caspr2 as a potential target in ASD pathogenesis [8]. Given the prevalence of these antibodies, we hypothesized that multiple pathogenic mechanisms for Caspr2 antibodies might exist. To investigate this proposition, we generated and characterized a panel of monoclonal anti-Caspr2 antibodies. While we were not able to determine actual affinities for Caspr 2 because of differential reactivity on each assay, the relative affinity based on the cell- based assay were P9C7 > PIIG7 > P6B2 > PBF4. Our findings reveal distinct differences in their specificity and pathogenicity, contributing to the heterogeneous nature of ASD.

IgG1 antibodies (P11G7 and P9C7) have divergent effects despite shared target domain

Both P11G7 and P9C7 target the discoidin domain of Caspr2, similar to Caspr2 autoantibodies from autoimmune encephalitis

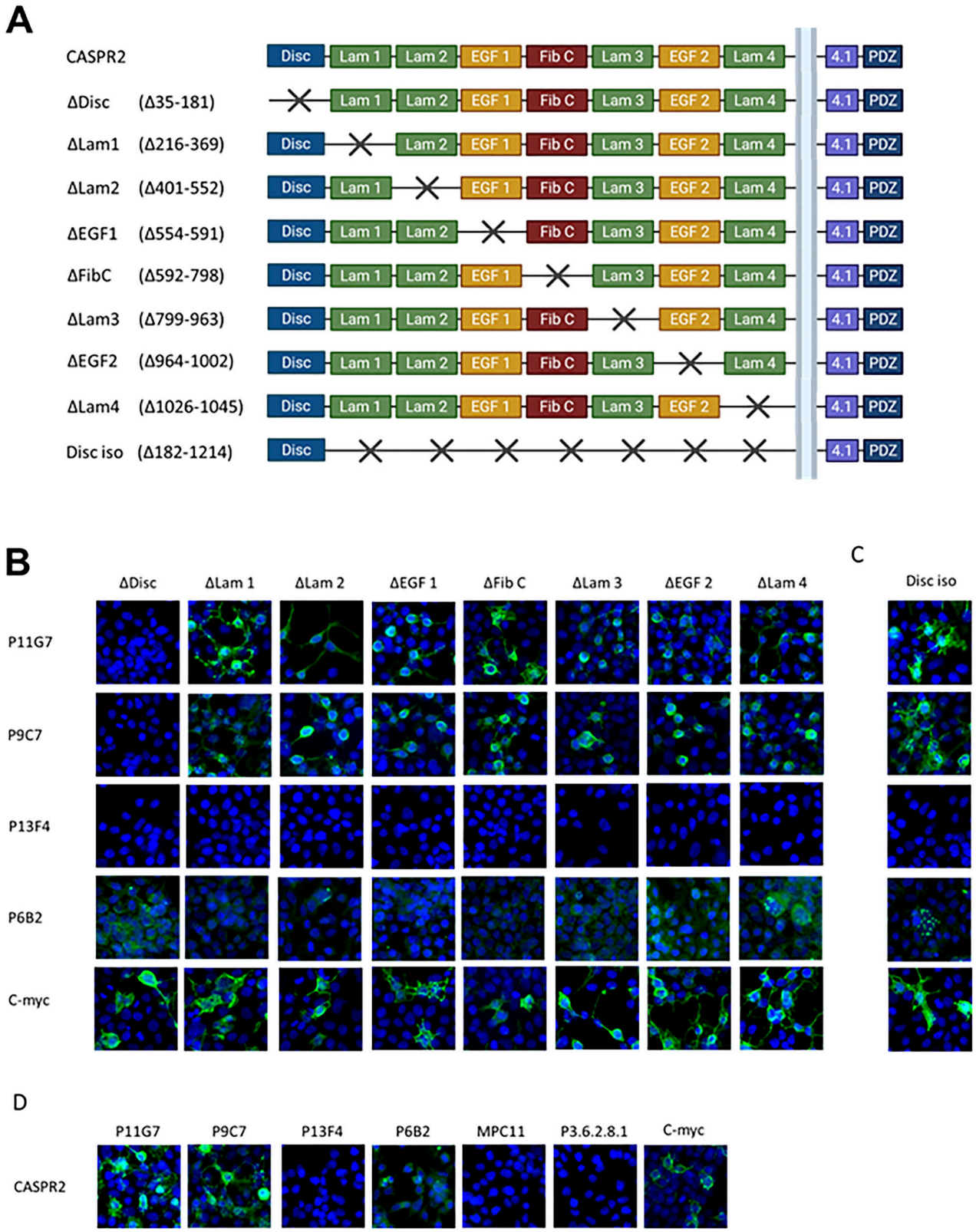

Fig. 3 Identification of anti-Caspr2 antibody target domains. A Caspr2 mutant constructs. The extracellular portion of Casor2 has 8 domains. The mutant constructs each missing one of the domains were previously generated [25]. Deletions are indicated by the respective amino acid positions (Δaa-aa). The Disc iso construct contains only the discoidin domain. **B** HEK293T cells were transfected with one of the Caspr2 mutant constructs for 48 h and incubated with each anti-Caspr2 antibody using live staining. P11G7 and P9C7 bind to all mutant constructs except the one missing the discoidin domain. P6B2 and P13F4 do not bind to any of the constructs. Isotype controls showed no binding to any construct. **C** P11G7 and P9C7 bind to the discoidin domain only construct. P13F4 and P6B2 do not bind to the discoidin domain only construct. **D** P11G7, P9C7, bind to Caspr2 transfected HEK293T cells. P6B2, P13F4 and the isotype controls do not.

patients that were found to predominantly bind the discoidin domain [25–27]. Despite this shared specificity, they induced distinct behavioral outcomes in male offspring following *in utero* exposure. While P11G7 exposure resulted in no overt behavioral changes, P9C7-exposed males exhibited both social interaction deficits and increased anxiety-like behavior. This divergence suggests that even antibodies targeting the same domain can differentially impact neurodevelopment, possibly through subtle variations in binding affinity, different epitopes within the same target domain, post-translational modifications of the Fc part, downstream signaling pathways, or by influencing distinct neuronal populations. The lack of dendritic changes in the CA1 and CA2 pyramidal neurons of P9C7-exposed males suggests that its effects on social behavior may involve other brain regions or processes.

IgG2b antibodies (P6B2 and P13F4) show distinct binding profiles and behavioral outcomes

P6B2 and P13F4 each exhibited distinct binding characteristics. P6B2 preferentially bound mouse Caspr2; P13F4showed binding to both human and mouse Caspr2 only in the absence of complex glycosylation, suggesting its epitope is masked in the native protein. *In utero* exposure to P6B2 resulted in social deficits in male offspring, accompanied by a significant reduction in dendritic length in the CA1 and CA2 pyramidal neurons, providing a potential anatomical correlate for the observed behavioral changes. In contrast, P13F4 exposure led to hyperactivity and increased anxiety-like behavior with no structural correlate in these dendrite measurements.

Potential mechanisms and the male bias in ASD

The distinct behavioral and anatomical changes induced by these antibodies suggest multiple pathways through which anti-Caspr2 antibodies might contribute to ASD-like phenotypes. The observed social deficits, particularly with P6B2 exposure, align with previous studies demonstrating reduced dendritic arborization in the hippocampus following *in utero* exposure to anti-Caspr2 antibodies [27, 33]. The hyperactivity observed in P13F4-exposed males, warrants further investigation into the specific neuronal circuits involved. While previous studies using homocysteine models have shown similar hyperactivity and dendritic changes [34], the distinct molecular targets suggest different mechanisms may be at play in our anti-Caspr2 model.

The male-specific vulnerability to anti-Caspr2 antibodies observed in our study is consistent with the male bias in ASD prevalence and previous findings in anti-Caspr2 models [10, 27]. This suggests a potential role for sex chromosomes in mediating this differential susceptibility [35], although the precise mechanisms remain to be elucidated.

A limitation of this study is the restricted scope of behavioral assessments conducted. Specifically, we did not incorporate ultrasonic vocalization tests that could have revealed potential communication deficits, nor did we assess targeted aggression, nest building capabilities, self-grooming patterns, or circling behaviors that might have indicated repetitive behaviors or stereotypies. We recognize that these additional behavioral measures would have provided a more complete understanding of the ASD-like phenotypes potentially induced by the newly generated anti-Caspr2 antibodies. Moving forward, we recommend incorporating these standardized assessments in future studies to better elucidate the full spectrum of behavioral effects associated with these antibodies and their potential contributions to ASD-like manifestations.

Conclusion

Our findings demonstrate that monoclonal anti-Caspr2 antibodies, even those targeting the same domain, can induce a range of phenotypes in social interaction, open field, and light-dark tasks in mice, highlighting the complexity of ASD pathogenesis. Further investigation into the specific molecular mechanisms underlying these diverse effects will be crucial for understanding the heterogeneity of ASD and developing targeted therapeutic strategies.

DATA AVAILABILITY

All data is included in the manuscript.

REFERENCES

1. Edition F. Diagnostic and statistical manual of mental disorders. Am Psychiatr Assoc. 2013;21:591–643.
2. Maenner MJ. Prevalence of autism spectrum disorder among children aged 8 years-autism and developmental disabilities monitoring network, 11 sites, United States, 2016. MMWR Surveill Summ. 2020;69:1–12.
3. Zeidan J, Fombonne E, Scorah J, Ibrahim A, Durkin MS, Saxena S, et al. Global prevalence of autism: a systematic review update. Autism Res. 2022;15:778–90.
4. Lord C, Bishop S, Anderson D, editors. Developmental trajectories as autism phenotypes. American Journal of Medical Genetics Part C: Seminars in Medical Genetics; Wiley Online Library 2015.
5. McLellan J, Kim DHJ, Bruce M, Ramirez-Celis A, Van de Water J. Maternal immune dysregulation and autism-understanding the role of cytokines, chemokines and autoantibodies. Front Psychiatry. 2022;13:834910. https://doi.org/10.3389/fpsyt.2022.834910.
6. Edmiston E, Ashwood P, Van de Water J. Autoimmunity, autoantibodies, and autism spectrum disorder. Biol Psychiatry. 2017;81:383–90.
7. Croen LA, Grether JK, Yoshida CK, Odouli R, Van de Water J. Maternal autoimmune diseases, asthma and allergies, and childhood autism spectrum disorders: a case-control study. Arch Pediatr Adolesc Med. 2005;159:151–7.
8. Brimberg L, Sadiq A, Gregersen P, Diamond B. Brain-reactive IgG correlates with autoimmunity in mothers of a child with an autism spectrum disorder. Mol Psychiatry. 2013;18:1171–7.
9. Atladottir HO, Pedersen MG, Thorsen P, Mortensen PB, Deleuran B, Eaton WW, et al. Association of family history of autoimmune diseases and autism spectrum disorders. Pediatrics. 2009;124:687–94.
10. Brimberg L, Mader S, Jeganathan V, Berlin R, Coleman T, Gregersen P, et al. Caspr2-reactive antibody cloned from a mother of an ASD child mediates an ASD-like phenotype in mice. Mol Psychiatry. 2016;21:1663–71.
11. Singer HS, Morris C, Gause C, Pollard M, Zimmerman AW, Pletnikov M. Prenatal exposure to antibodies from mothers of children with autism produces neurobehavioral alterations: a pregnant dam mouse model. J Neuroimmunol. 2009;211:39–48.
12. Braunschweig D, Ashwood P, Krakowiak P, Hertz-Picciotto I, Hansen R, Croen LA, et al. Autism: maternally derived antibodies specific for fetal brain proteins. Neurotoxicology. 2008;29:226–31.
13. Ramirez-Celis A, Becker M, Nuno M, Schauer J, Aghaeepour N, Van de Water J. Risk assessment analysis for maternal autoantibody-related autism (MAR-ASD): a subtype of autism. Mol Psychiatry. 2021;26:1551–60. https://doi.org/10.1038/s41380-020-00998-8.
14. Zimmerman AW, Connors SL, Matteson KJ, Lee LC, Singer HS, Castaneda JA, et al. Maternal antibrain antibodies in autism. Brain Behav Immun. 2007;21:351–7. https://doi.org/10.1016/j.bbi.2006.08.005.
15. Croen LA, Braunschweig D, Haapanen L, Yoshida CK, Fireman B, Grether JK, et al. Maternal mid-pregnancy autoantibodies to fetal brain protein: the early markers for autism study. Biol Psychiatry. 2008;64:583–8. https://doi.org/10.1016/j.biopsych.2008.05.006.
16. Bruce MR, Couch ACM, Grant S, McLellan J, Ku K, et al. Altered behavior, brain structure, and neurometabolites in a rat model of autism-specific maternal autoantibody exposure. Mol Psychiatry. 2023;28:2136–47. https://doi.org/10.1038/s41380-023-02020-3. PubMed PMID: 36973347; PMCID: PMC10575787 has a UC Davis-based startup company focusing on the development of the MAR-ASD autoantibody profile as a risk assessment for a child developing ASD. All other authors have no conflicts of interest to declare.
17. McLellan J, Kim DH, Bruce M, Ramirez-Celis A, Van de Water J. Maternal immune dysregulation and autism–understanding the role of cytokines, chemokines and autoantibodies. Front Psychiatry. 2022;13:834910.
18. Jones KL, Pride MC, Edmiston E, Yang M, Silverman JL, Crawley JN, et al. Autism-specific maternal autoantibodies produce behavioral abnormalities in an endogenous antigen-driven mouse model of autism. Mol Psychiatry. 2020;25:2994–3009. https://doi.org/10.1038/s41380-018-0126-1.
19. Ramirez-Celis A, Croen LA, Yoshida CK, Alexeeff SE, Schauer J, et al. Maternal autoantibody profiles as biomarkers for ASD and ASD with co-occurring intellectual disability. Mol Psychiatry. 2022;27:3760–7. https://doi.org/10.1038/s41380-022-01633-4. PubMed PMID: 35618885; PMCID: PMC9708563 company to

develop this technology for commercial use. The remaining authors have no conflicts of interest.

20. Bruce MR, Jones KL, Vernon AC, Silverman JL, Crawley JN, Ellegood J, et al. Sexually dimorphic neuroanatomical differences relate to ASD-relevant behavioral outcomes in a maternal autoantibody mouse model. Mol Psychiatry. 2021;26:7530–7. https://doi.org/10.1038/s41380-021-01215-w.
21. Dalton P, Deacon R, Blamire A, Pike M, McKinlay I, Stein J, et al. Maternal neuronal antibodies associated with autism and a language disorder. Ann Neurol. 2003;53:533–7. https://doi.org/10.1002/ana.10557.
22. McLellan J, Iosif AM, Cichewicz K, Canales C, Rahbarian D, Corea M, et al. Gestational autoantibody exposure impacts early brain development in a rat model of MAR autism. Mol Psychiatry. 2025;30:3018–28. https://doi.org/10.1038/s41380-025-02907-3. PubMed PMID: 39929953; PMCID: PMC12185337 autoantibody technology and has founded a UC Davis startup company to develop this technology for commercial use. Ethics approval: All animal procedures were performed in accordance with the relevant guidelines and regulations and were approved by the University of California, Davis Institutional Animal Care and Use Committee.
23. Varea O, Martin-de-Saavedra MD, Kopeikina KJ, Schürmann B, Fleming HJ, Fawcett-Patel JM, et al. Synaptic abnormalities and cytoplasmic glutamate receptor aggregates in contactin associated protein-like 2/Caspr2 knockout neurons. Proc Natl Acad Sci. 2015;112:6176–81.
24. Peñagarikano O, Abrahams BS, Herman EI, Winden KD, Gdalyahu A, Dong H, et al. Absence of CNTNAP2 leads to epilepsy, neuronal migration abnormalities, and core autism-related deficits. Cell. 2011;147:235–46.
25. Poot M. Connecting the CNTNAP2 networks with neurodevelopmental disorders. Mol Syndromol. 2015;6:7–22.
26. Anderson GR, Galfin T, Xu W, Aoto J, Malenka RC, Sudhof TC. Candidate autism gene screen identifies critical role for cell-adhesion molecule CASPR2 in dendritic arborization and spine development. Proc Natl Acad Sci USA. 2012;109:18120–5. https://doi.org/10.1073/pnas.1216398109.
27. Bagnall-Moreau C, Huerta PT, Comoletti D, La-Bella A, Berlin R, Zhao C, et al. In utero exposure to endogenous maternal polyclonal anti-Caspr2 antibody leads to behavioral abnormalities resembling autism spectrum disorder in male mice. Sci Rep. 2020;10:14446.
28. Rubio-Marrero EN, Vincelli G, Jeffries CM, Shaikh TR, Pakos IS, Ranaivoson FM, et al. Structural characterization of the extracellular domain of CASPR2 and insights into its association with the novel ligand Contactin1. J Biol Chem. 2016;291:5788–802. https://doi.org/10.1074/jbc.M115.705681.
29. Yelton DE, Scharff MD. Monoclonal Antibodies: Antibody-forming hybrids—or hybridomas—have made it possible to produce virtually unlimited supplies of a wide variety of antibodies. Am Sci. 1980;68:510–6.
30. Nestor J, Arinuma Y, Huerta TS, Kowal C, Nasiri E, Kello N, et al. Lupus antibodies induce behavioral changes mediated by microglia and blocked by ACE inhibitors. J Exp Med. 2018;215:2554–66. https://doi.org/10.1084/jem.20180776.
31. Carroll KR, Mizrachi M, Simmons S, Toz B, Kowal C, Wingard J, et al. Lupus autoantibodies initiate neuroinflammation sustained by continuous HMGB1:RAGE signaling and reversed by increased LAIR-1 expression. Nat Immunol. 2024. https://doi.org/10.1038/s41590-024-01772-6.
32. van Hoof S, Kreye J, Cordero-Gómez C, Hoffmann J, Reincke SM, Sánchez-Sendin E, et al. Human cerebrospinal fluid monoclonal CASPR2 autoantibodies induce changes in electrophysiology, functional MRI, and behavior in rodent models. Brain Behav Immun. 2024;122:266–78.
33. Coutinho E, Menassa DA, Jacobson L, West SJ, Domingos J, Moloney TC, et al. Persistent microglial activation and synaptic loss with behavioral abnormalities in mouse offspring exposed to CASPR2-antibodies in utero. Acta Neuropathol. 2017;134:567–83. https://doi.org/10.1007/s00401-017-1751-5.
34. De la Torre-Iturbe S, Vázquez-Roque RA, De la Cruz-López F, Flores G, Garcés-Ramírez L. Dendritic and behavioral changes in rats neonatally treated with homocysteine; A proposal as an animal model to study the attention deficit hyperactivity disorder. J Chem Neuroanat. 2022;119:102057.
35. Gata-Garcia A, Porat A, Brimberg L, Volpe BT, Huerta PT, et al. Contributions of sex chromosomes and gonadal hormones to the male bias in a maternal antibody-induced model of autism spectrum disorder. Front Neurol. 2021;12:721108.

ACKNOWLEDGEMENTS

We thank Joe Gallagher for help with behavioral assays. Funding was provided by the National Institute of Health (NIH) grant 5P01AI073693 (to BD). PH acknowledges the Department of Defense (DOD) impact award W81XWH1910759. PR received funding from the German Research Foundation (DFG) grants FOR3004, PR1274/9-1, clinical research unit 5023/1 'BECAUSE-Y' (project number 504745852), the Helmholtz Association (HIL-A03 BaoBab), and the German Federal Ministry of Education and Research (Connect-Generate 16GW0279K). JK was supported by the Berlin Institute of Health at Charité Clinician Scientist program and received funding from German Research Foundation (DFG) grant FOR3004 (project number 415914819).

AUTHOR CONTRIBUTIONS

JS designed and performed experiments and helped write the paper; RG performed the histological experiments and helped with the statistics; BV supervised the histology and helped write the paper; PH supervised the behavioral studies and helped write the paper; LB helped analyze the behavioral data and write the paper; BS helped with the histological analysis; SvH, JK, and HP performed experiments and helped write the paper, BD designed, supervised the experiments and helped write the paper.

COMPETING INTERESTS

The authors declare no competing interests.

ETHICS

All experiments were approved by the IACUC at the Feinstein Institute.

ADDITIONAL INFORMATION

Supplementary information The online version contains supplementary material available at https://doi.org/10.1038/s41398-025-03677-w.

Correspondence and requests for materials should be addressed to Betty Diamond.

Reprints and permission information is available at http://www.nature.com/reprints

Publisher's note Springer Nature remains neutral with regard to jurisdictional claims in published maps and institutional affiliations.